EVALUATION OF A FORTY-YEAR OLD T.Y. LIN DESIGNED ELLIPTICAL POST-TENSIONED CABLE-SUPPORTED ROOF

Randall W. Poston
Principal, WDP & Associates, Inc.
Austin, Texas, USA
E-mail: rposton@wdpa.com

Introduction

A structural evaluation of the roof and post-tensioning system and an assessment of the current integrity of the roof of the Norick Arena located on the State Fair Grounds in Oklahoma City, Oklahoma was conducted.

The roof of the Norick Arena is an elliptical post-tensioned concrete roof system with a major axis of about 400 ft. and a minor axis of about 320 ft. The original design was performed by T.Y. Lin and Associates using three-dimensional load-balancing for full dead load and live load. Although elliptical in shape, the post-tensioning tendons form an inverted cable net in which precast concrete panels were suspended and subsequently made monolithic by casting thickened grout beams to form a structural roof that is a relatively thin, monolithic shell membrane.

The roof system is supported by a reinforced concrete compression ring, which in turn is supported by rectangular reinforced concrete columns. Stub tendons are cast into the ring beam and then coupled to the main suspended roof tendons. The post-tensioning is an unbonded, wire-based, button-headed system covered with mastic and placed in a waterproof paper, which essentially acts as a duct. The major axis tendon ducts are 2-1/4 in. in diameter, whereas the minor axis tendon ducts are 1-1/4 in. in diameter. Typical details of the post-tensioning system are shown in Figure 1.

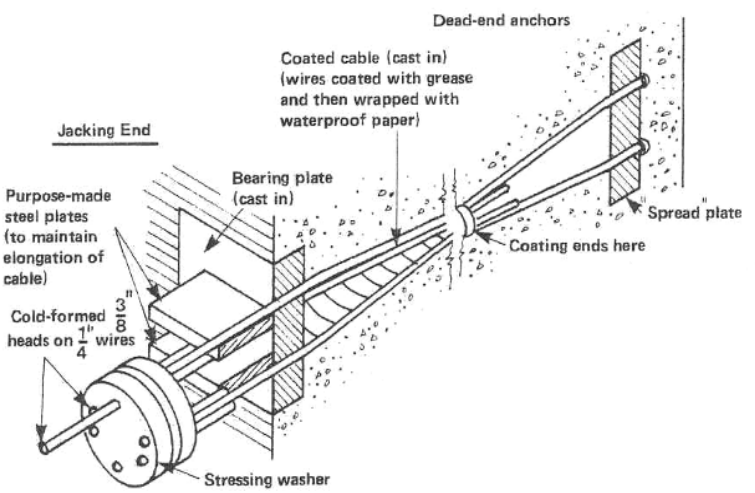

Figure 1. Post-tensioning system details from literature.

M. Pandey et al. (eds), Advances in Engineering Structures, Mechanics & Construction, 343–354.

The arena was constructed in 1965 using a four-stage post-tensioning process with the monolithic concrete membrane stressed at the third stage. The post-tensioning was primarily staged to mitigate cracking in the compression ring. The fourth stage post-tensioning was applied to balance about 12 psf of live load (Lin and Burns, 1981). Figure 2 is an overall view of the arena from ground.

Figure 2. General view of arena exterior.

This paper will summarize the investigation of the post-tension roof of the Norick Arena roof. Results from field investigation procedures and from structural analyses are presented in the context of assessment of current integrity.

Field Evaluation Procedures

The arena roof was evaluated using different nondestructive techniques consisting of surface penetrating radar (SPR) scanning, impact-echo (IE) testing and infrared thermography (IT). A geometry survey of the roof was also conducted, as well as a general visual inspection of the roof, compression ring beam and columns. Invasive probe openings were made at select post-tensioning components in order to assess the general condition of the post-tensioning system.

Geometry Survey

A differential elevation survey (see Figure 3) was conducted to determine the difference in elevation between the edge of the ring beam and various points near the center of the roof, including the center. The difference in the ring beam elevation and the PT at the center of the roof is the “sag” of the roof. Column deformation was determined using a laser level and a laser distance meter. These measurements of the roof sag and column deformation were made to compare to theoretical values computed from structural analyses.

Figure 3. Surveying to determine roof sag.

Invasive Probing and Visual Observations

There are no direct, nondestructive means to assess the condition of post-tensioning (PT) systems. The most direct way of examining tendon condition is to conduct selected probing at the anchorages, couplers, and other strategic locations along the tendon trajectory.

Visual observations were conducted at select probe openings of the post-tensioning system to document conditions. This included documentation of signs of corrosion of PT components, prestressing wire pitting, degradation of the "sisal craft" paper used for the tendon duct, and condition of the corrosion-protection mastic. Photographs were made to document conditions, and where appropriate, measurements were taken of pertinent details such as cover depth.

Nondestructive Testing

Various nondestructive testing (NDT) methods including surface penetrating radar (SPR), impact-echo (IE) and infrared thermography (IT) were utilized to assess various aspects of the concrete deck conditions. For brevity, only general results from the NDT will be presented.

Analysis

Structural System

The roof of the Norick Arena is shaped as an elliptic-paraboloid. The plan view of the roof is an ellipse with major and minor axes of about 400 ft. and 320 ft., respectively. The cross sections of the roof on planes parallel to the planes containing the major and minor axes of the ellipse are also parabolas. The deepest parabolas intersect at the center of the roof where the difference in elevation with respect to its perimeter was designed to be 17 ft. 3 in. from examination of the structural

drawings. Figure 4 shows an overall plan view of the roof structural system and the reinforced concrete columns supporting it, and the section of the roof along the major axis of the ellipse. A concrete ring beam connects the columns and the structural roof. The PT tendons are anchored into the ring beam. Although the dimensions of the columns vary somewhat, the predominant dimensions are 18 in. by 58.5 in. with the strong axis parallel to the axis of the ring beam and a height of 62 ft. The ring beam is approximately 108 in. wide by an average 36 in. in depth.

The roof structural system consists of an arrangement of essentially "T-beams" spaced 10 ft. on center located on planes parallel to the planes containing both the major and minor axes of the elliptic-paraboloid. These beams consist of 9 ft. 7 in. square precast concrete panels of 3 in. thickness. The equivalent section used in the analysis is shown in Figure 6. The surface of the roof is covered by insulating and roofing material protecting it from weather. There were two roofing systems that had been applied over the 40-year history of the arena. The outermost layer of roofing insulation is a closed-cell foam and has a variable thickness ranging from about 4 to 6 in. It is somewhat thicker at the center of the roof. This layer prevented a direct visual evaluation of the current structural condition of the concrete surface of the roof other than at limited exposed areas of the probe openings.

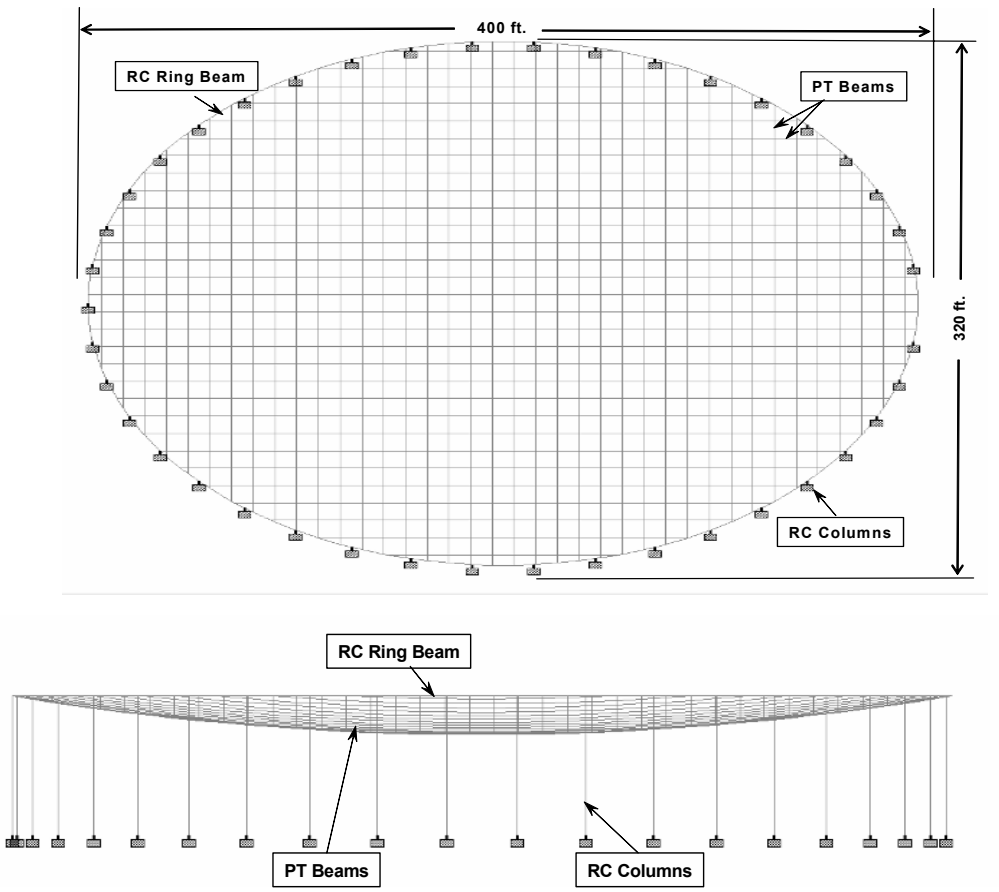

Figure 4. Roof plan view (top) and section along major axis (middle).

Material Properties

The material properties considered in the analysis were, f'_c, concrete compressive strength equal to 4000 psi. The prestressing steel wires that comprise the post-tensioning tendons had an ultimate strength, f_{pu}, equal to 240 ksi.

Post-tensioning Effects

The post-tensioning tendons were modeled using equivalent load effects. The effective anchorage force of each tendon after losses was determined to be 352 kips for the strong axis tendons and 224 kips for the minor axis tendons. The equivalent uniform uplift of the tendons was determined to be 68 psf by using the simplified load balancing model. This assumes that the effective stress, f_{se}, in the tendons considering time-dependent losses was equal to 0.6 f_{pu}, which is 144 ksi. Figure 5 shows a simplified load-balancing model with two "super tendons" along the major and minor axes to represent all post-tensioning tendons in the structural roof.

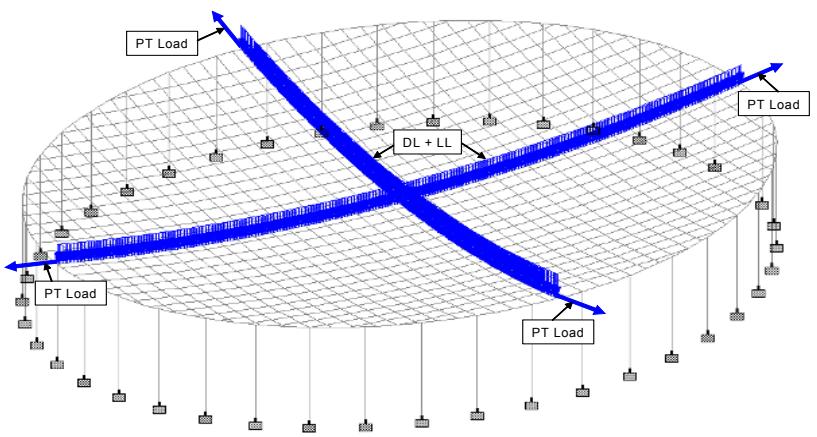

Figure 5. Equivalent force system of PT tendons.

The roof system was modeled with equivalent post-tensioned beams forming a 10 ft. waffle grid. The equivalent section that includes the precast panels is shown in Figure 6.

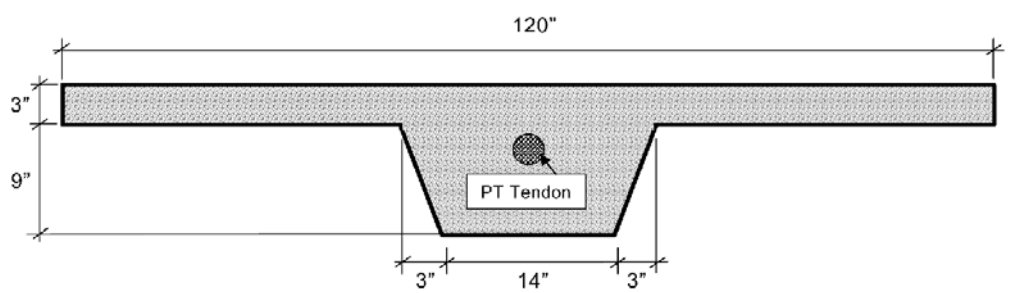

Figure 6. Equivalent roof post-tension beam cross section detail.

Loads

The roof system of the Norick Arena was analyzed for gravity loads. The dead load of the precast waffle deck section with its original built-up roofing was determined to be approximately 56 psf.

There are currently two types of roofing materials on the roof. There is an older built-up membrane and asphalt system covered by a newer sprayed-foam system. This sprayed-foam system is the principal weather-proofing. The thickness of the foam was measured to be about 4 in. as measured at select probe openings. At the center of the roof, the foam has been built up to about 6 to 10 in. to provide a slope for drainage. The average weight of this existing foam roofing material was determined to be 3 psf.

The snow load for the Norick Arena roof as determined from ASCE 7 (ASCE 2002) is 7 psf.

Load Cases

The structural condition of the post-tensioned concrete roof is important to assess if corrosion or other forms of deleterious phenomena have affected its integrity. In general, as a post-tensioned structure ages, its post-tensioning system experiences normal losses induced by relaxation of the steel tendons and by creep and shrinkage in the concrete. In addition, the concrete may experience cracking of some degree, which in turn affects its stiffness. Significant deterioration of the PT tendons due to corrosion would manifest as a loss of effective prestress and the roof's overall ability to carry load.

There were several variations of the structural model and load cases that were examined for comparison purposes with field measurements and to assess the sensitivity of various parameters on the roof behavior. Table 1 summarizes the various analysis cases that were examined.

Table 1. Summary of Analysis Cases.

Case No.	Description	Column Inertia	Long-term Modulus	DL (psf)	LL (psf)
1	Base case.	I_g	No	56	12
2	Considers cracked columns. Added 3 psf due to foam roof material.	0.5 I_g	No	59	0
3	Considers time-dependent effects on concrete modulus.	0.5 I_g	Yes	59	0
4	Determine LL to produce $6\sqrt{f_c'}$ tension fiber stress.	0.5 I_g	Yes	59	Varies 0 to 19
5	Determine effect of 10% loss of prestress due to deterioration.	0.5 I_g	Yes	59	0
6	Determine effect of 25% loss of prestress due to deterioration.	0.5 I_g	Yes	59	0
7	Determine effect of 50% loss of prestress due to deterioration.	0.5 I_g	Yes	59	0

Base Case

This model assumed that the structural elements were uncracked, and therefore, assumed gross section properties.

Column Cracking

This model assumed that the columns supporting the roof were cracked based on an analysis of the cracking moment. Accordingly, the moment-of-inertia was assumed to be 0.5 I_{gross}.

Time-Dependent Effects

The time-dependent effects of creep and shrinkage in concrete were modeled using the ACI Committee 209 effective modulus approach (ACI 209, 1997) as follows:

$$E_{t=\infty} = \frac{E_{t=28days}}{1+\phi}$$

where $E_{t=\infty}$ = *long-term modulus of elasticity*

$$E_{t=28days} = 57000\sqrt{f_c'}$$

and ϕ = *time- factor; this case equal to 1.5*

Field Investigation Results

There were no visual observations made of the roof system that indicated that there has been a loss of integrity. There were observations made that selected columns have experienced some corrosion-related deterioration, but were not impacting the roof's integrity.

Visual Observations

Prestressing Wires.

Figure 7 shows a typical condition of the prestressing wires exposed at each tendon opening. The wires generally appeared to be in good condition with only evidence of minor surface corrosion. The dark color of the wires is discoloration principally from the mastic. This minor surface corrosion did not appear "fresh" as would have been evidenced by a bright orange corrosion product. There were no significant corrosion pits indicative of area loss.

The paper wrap, which acts as the unbonded PT duct, has experienced some deterioration as observed in Figure 7. The bitumen mastic that was used to protect the wires from corrosion was variable in thickness and coverage. However, as long as the roofing material prevents water intrusion, the deterioration of the paper duct and presence variable mastic is not considered overly significant.

Figure 7. Typical condition of prestressing wires.

Coupler.

The condition of the exposed coupler along the strong axis tendon is observed in Figure 8. There was little evidence of corrosion of the metal duct that was split open to observe the coupler, threaded rod or anchors. Also note that the "buttons" of each wire are intact and show no evidence of corrosion.

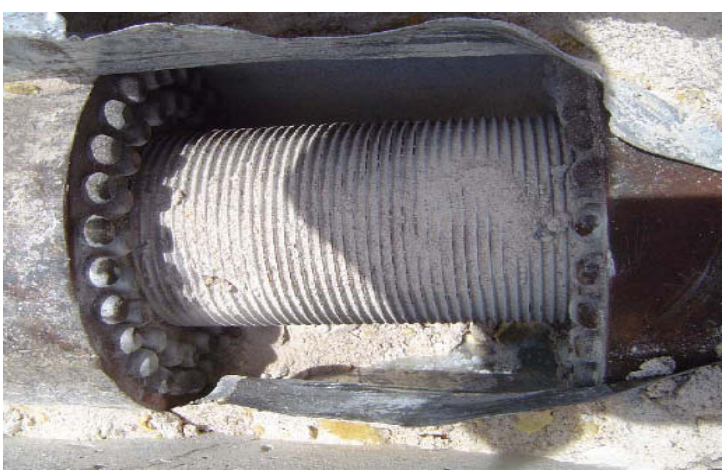

Figure 8. Condition of exposed coupler.

Anchorage.

Figure 9 shows the representative condition observed at the exposed anchorages of the PT tendons. The field investigation at the selected anchorages clearly indicated that there has been no significant corrosion of the prestressing wires, bearing plate or transfer plates.

Figure 9. Typical condition of exposed anchorage.

Geometry Survey

Based on the differential survey conducted, the roof sag as measured from the edge of the roof to the center was between approximately 17 ft. 4 in. and 17 ft. 8 in. The range is given since the exact thickness of the roof foam at these locations is not known. This measured value was compared to computed values from analysis under dead load only since at the time of the measurements there were no superimposed live loads.

NDT

Impact-echo testing revealed that the precast concrete panels were solid with no signs of corrosion-related deterioration. Infrared thermography indicated that the concrete deck surface was being adequately protected from moisture by the roofing.

Structural Analysis Results

The structural model for the Norick Arena was used to study the structural behavior of the structure under various load combinations and conditions. The implications of these results in the context of selected field measurements are presented. The theoretical sag at the middle is taken as 17 ft. 3 in. as determined from the original structural drawings. All deflection results are presented from this benchmark sag. Table 2 summarizes the results from the various analyses.

Case 1

This base model was considered in order to understand the expected behavior of the roof structure from the original design. This model considered a dead load of 56 psf, live load of 12 psf and the post-tensioning as fully effective. Gross section properties were considered for the column sections.

The analysis shows that the maximum downward deflection at the middle of the roof is about 2.1 in. below the benchmark sag. It was found that the columns developed bending moments in excess of the cracking moment.

Table 2. Summary of Analysis Results.

Case No.	**Column Inertia**	**Long-term Modulus**	**DL (psf)**	**LL (psf)**	**Additional PT Losses from $f_{ps} = 0.6\ f_{pu}$ (%)**	**Center Deflection from Theoretical Sag (17 ft. 3 in.), Positive Downward (in)**
1	I_g	No	56	12	0	2.1
2	0.5 I_g	No	59	0	0	1.3
3	0.5 I_g	Yes	59	0	0	3.2
4	0.5 I_g	Yes	59	Varies 0 to 19	0	Varies 3.2 to 7.5
5	0.5 I_g	Yes	59	0	10	4.2
6	0.5 I_g	Yes	59	0	25	5.6
7	0.5 I_g	Yes	59	0	50	8.1

Case 2

This case closely reflects Case 1, except that the column stiffness was reduced to 50% of that based on gross section properties to account for cracking. The field observations presented previously confirmed the presence of flexural cracks. Also, the dead load was increased to reflect the weight of the foam roof. The live load was removed to reflect conditions when field measurements were taken.

The field measurements indicate that the present roof sag is in the range of about 17 ft. 4 in. to 17 ft. 8 in. This is an increase in sag of 1 in. to 5 in. The computed value of Case 2 is in between these values.

Case 3

As part of the various analyses of the structure, this model considered long-term effects. This model is based on Case 2 with the addition of long-term effects. These effects are modeled by reducing the elastic modulus of the structural members by a factor corresponding to the long-term conditions

expected on the structure. In this case, a factor of 0.4 was computed, indicating that for long–term conditions, the effective elastic modulus is about 40% of its original value. The structural analysis yields an increase in downward deflection of 3.2 in. The sag in the center of the roof increases by only about 2 in. considering time-dependent effects. The computed deflection is virtually in between the range of measured values. This strongly suggests that there has been no measurable loss in prestressing of the post-tensioning tendons.

Case 4

The ACI 318 Building Code (ACI 318, 2005) requires that a post-tensioned structure limit tension stress to $6\sqrt{f_c'}$ under full service loads. Case 4 was conducted to determine the level of live load acting on the structure needed to exceed the limiting tension stress. This value would be one possible index in determining the current load rating of the roof. Analyses showed this value to be about 19 psf. Under this loading and under similar conditions as in Case 3, the maximum downward deflection increases by 7.5 in. from the benchmark sag.

Cases 5 to 7

These analyses consider additional losses in the post-tensioning tendons due to some form of deterioration such as corrosion or other factors that might result in a partial loss of prestressing. These additional losses considered were 10%, 25% and 50%, respectively. These losses were applied to the same analysis model and loads of Case 3. The results are summarized in Figure 10. This graph shows that considering 0% losses in the post-tensioning, the deflection in the middle of the roof is about 3.2 in., whereas, 50% losses in the effective post-tensioning stress results in a deflection of 8.1 in. The analysis indicates that the center deflection of the roof is not overly sensitive to assumed losses in the post-tensioning from some form of deterioration. The increase in roof deflection is linear with the percentage of prestressing losses.

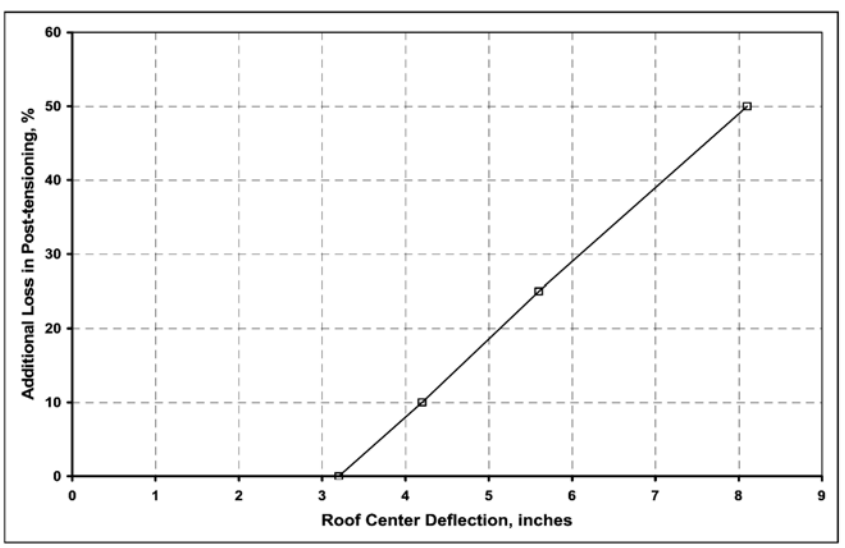

Figure 10. Deflection at middle of roof compared to assumed additional losses in post-tensioning.

Collapse Conditions

As a perspective of the conditions that would result in the "collapse" of the roof under its existing weight, a collapse analysis indicates that, on average, 65% of the post-tensioning would have to be lost from the effects of corrosion or as a result of some type of catastrophic event. The resulting increase in sag would be about 10 in.

Conclusions

A field evaluation and structural assessment was conducted for the post-tensioned concrete roof of the Norick Arena, which was designed by T.Y. Lin in l965. There were no signs of significant deterioration that would indicate that the structural roof system has been compromised in its 40-year life thus far. It was determined that the roof will continue to safely carry the intended code-required loads as long as the roofing material is adequately maintained to mitigate ingress of water and as long as the roof drains are maintained.

The analysis indicates that the post-tensioning system was designed to balance a total load of about 68 psf. The present dead load of the roof is approximately 59 psf. Thus, the allowable additional live load from purely a load-balancing perspective is 9 psf. This exceeds the current snow load of 7 psf.

References

ACI Committee 209 (1997), "ACI 209R-92: Prediction of Creep, Shrinkage and Temperature Effects in Concrete", American Concrete Institute, Detroit, MI, 47 pp.

ACI Committee 318 (2005), "ACI 318-05: Building Code Requirements for Structural Concrete and ACI 318R-05: Commentary", American Concrete Institute, Detroit, MI, 430 pp.

ASCE (2002), "Minimum Design Loads for Buildings and Other Structures", American Society of Civil Engineers, Reston, VA, 376 pp.

Lin, T.Y. and Burns, N.H. (1981), "Design of Prestressed Concrete Structures", Third Edition, John Wiley & Sons, New York, NY, 646 pp.